Ecology and Evolution

Open Access

# Global remote sensing of water–chlorophyll ratio in terrestrial plant leaves

Keiji Kushida

Center for Far Eastern Studies and Graduate School of Science and Engineering (Science), University of Toyama, 3190 Gofuku, Toyama, 930-8555, Japan

**Keywords**
Leaf area index, leaf chlorophyll concentration, leaf water concentration, radiative transfer, remote sensing.

**Correspondence**
Keiji Kushida, Center for Far Eastern Studies and Graduate School of Science and Engineering (Science), University of Toyama, 3190 Gofuku, Toyama 930-8555, Japan.
Tel: +81 76 445 6648; Fax: +81 76 445 6549; E-mail: kkushida@sci.u-toyama.ac.jp

**Funding Information**
This study was supported by the Grant-in-Aid for Scientific Research (C),20510001, 2008, from the Japan Ministry of Education, Science, Sports and Culture (MEXT) and the Arctic Research Projects using the IARC-JAXA Information System of the Japan Aerospace Exploration Agency (JAXA).

Received: 9 May 2012; Revised: 23 July 2012; Accepted: 26 July 2012

*Ecology and Evolution* **2012; 2(10): 2544–2551**

doi: 10.1002/ece3.361

## Abstract

I evaluated the use of global remote sensing techniques for estimating plant leaf chlorophyll $a + b$ ($C_{ab}$; $\mu$g cm$^{-2}$) and water ($C_w$; mg cm$^{-2}$) concentrations as well as the ratio of $C_w/C_{ab}$ with the PROSAIL model under possible distributions for leaf and soil spectra, leaf area index (LAI), canopy geometric structure, and leaf size. First, I estimated LAI from the normalized difference vegetation index. I found that, at LAI values <2, $C_{ab}$, $C_w$, and $C_w/C_{ab}$ could not be reliably estimated. At LAI values >2, $C_{ab}$ and $C_w$ could be estimated for only restricted ranges of the canopy structure; however, the ratio of $C_w/C_{ab}$ could be reliably estimated for a variety of possible canopy structures with coefficients of determination ($R^2$) ranging from 0.56 to 0.90. The remote estimation of the $C_w/C_{ab}$ ratio from satellites offers information on plant condition at a global scale.

## Introduction

Leaf chlorophyll $a + b$ ($C_{ab}$; $\mu$g cm$^{-2}$), dry matter ($C_m$; mg cm$^{-2}$), and water ($C_w$; mg cm$^{-2}$) concentrations provide information on plant physiological status and ecosystem functioning (e.g., terrestrial heat, water, and $CO_2$ balances) (Zarco-Tejada et al. 2003). Nevertheless, global remote estimates of vegetation status mainly focus on leaf area index (LAI; Garrigues et al. 2008), fraction of absorbed photosynthetically active radiation (FAPAR; Running et al. 2004), phenology (Zhang et al. 2006), leaf clumping (Chen et al. 2005), and vegetation height (Simard et al. 2011).

Site-specific studies have clarified the relationships between plant canopy spectral reflectance and $C_{ab}$ (Zarco-Tejada et al. 2004; Gitelson et al. 2005; Darvishzadeh et al. 2012; Si et al. 2012), $C_m$, (Fourty and Baret 1997) and $C_w$ (Bowyer and Danson 2004; De Santis et al. 2006; Zarco-Tejada et al. 2003). However, global or regional relationships between these factors are not clearly understood because other characteristics of the plant canopy impact those relationships. In this note, I evaluated the use of global remote sensing techniques for estimating $C_{ab}$, $C_m$, $C_w$, and the $C_w/C_{ab}$ ratio using the PROSAIL model (Jacquemoud et al. 2009) at varying possible distributions of leaf and soil spectra, LAI, canopy geometric structure, and leaf size.

**Table 1.** Input parameters for the PROSAIL model.

| | Unit | Value/function |
|---|---|---|
| $\ln(C_{ab})$ | $\mu$g cm$^{-2}$ | $N(3.79, 0.35^2)$* |
| $\ln(C_m)$ | mg cm$^{-2}$ | $N(1.57, 0.42^2)$* |
| $\ln(C_w)$ | mg cm$^{-2}$ | $N(2.32, 0.47^2)$* |
| The coefficient of correlation between $\ln(C_{ab})$ and $\ln(C_m)$ | – | 0.56 |
| The coefficient of correlation between $\ln(C_w)$ and $\ln(C_{ab})$ or $\ln(C_m)$ | – | 0 |
| The parameter characterizing the leaf mesophyll structure, $N$ | – | $N(1.7, 0.2^2)$* |
| Soil reflectance | – | JHU-SL based statistic model |
| Clumping index, $\Omega$ | – | Any (fixed at 0.7 for LAI calculation) |
| Leaf angle distribution, LAD | – | Erectophile, spherical, plagiophile, uniform, extremophile, and planophile |
| Canopy hotspot parameter, $S_l$ | – | 0.0001, 0.001, 0.01, and 0.1 |
| Leaf area index, $LAI = LAI_r \cdot \Omega$ | – | 0–10 ($10^{-6}$ interval) |
| Solar incident zenith angle, $\theta_s$ | ° | 25 and 50 |
| View zenith angle, $\theta_v$ | ° | 0 |
| Solar illumination specular ratio, $r_{sd}$ | – | Constant (0.81, 0.91, 0.95, 0.98, and 1.0 in MODIS bands 3, 4, 1, 2, and 5–7) |
| Error function of the atmospheric correction | – | $N(0, (0.005 + 0.05\rho)^2)$* |

*$N(\mu,\sigma^2)$ denotes the normal distribution with mean $\mu$ and variance $\sigma^2$.

## Materials and Methods

I used the PROSAIL model, which is a combination of the SAIL (Verhoef 1984) and PROSPECT (Jacquemoud and Baret 1990) models, for calculating the relationships between the top-of-the-atmosphere (TOA) canopy spectral reflectance and $C_{ab}$, $C_m$, $C_w$, and $C_w/C_{ab}$. The input parameters of the PROSAIL model are listed in Table 1, and I noted TOA canopy spectral reflectance from the model outputs.

I calculated the relationship between the normalized difference vegetation index (NDVI) and LAI (m$^2$ m$^{-2}$) following Kushida and Yoshino (2010). I used the TOA canopy spectral reflectance values at the Moderate Resolution Imaging Spectroradiometer (MODIS) red (620–670 nm; $R_R(\%)$) and near infrared (841–876 nm; $R_{NIR}(\%)$) bands to calculate NDVI as follows:

$$\mathrm{NDVI} = \frac{R_{NIR} - R_R}{R_{NIR} + R_R} \quad (1)$$

For the estimated LAI value ranges of 0.95–1.05, 1.95–2.05, 2.95–3.05, 3.95–4.05, 4.95–5.05, 5.95–6.05, and 6.95–7.05, I calculated the relationships between canopy spectral reflectance and $C_{ab}$, $C_m$, $C_w$, and $C_w/C_{ab}$.

I assumed that $C_{ab}$, $C_m$, and $C_w$ had lognormal distributions based on the leaf optical properties experiment (LOPEX93), which provides values for leaf pigment and water content of 70 leaf samples that represent approximately 50 species of woody and herbaceous plants (Hosgood et al. 1995). The means and standard deviations (SD) of the lognormal distributions and the correlations and ranges of the variables were also determined using the data values in LOPEX93. All calculations were carried out under variable soil spectrum conditions. The soil reflectance distribution for each of the bands was assumed to be lognormal or normal, based on the Johns Hopkins University Spectral Library (JHU-SL; Baldridge et al. 2009). The means and SD of the distributions and the correlations and ranges of the variables were determined using the data values in JHU-SL.

The clumping index ($\Omega$; Chen et al. 2005) was incorporated in the model by setting the parameter at 0.7 to express the leaf clumping effect. Using this parameter, I adjusted the LAI value such that, in a plant canopy with an initial LAI value of $LAI_r$ and an $\Omega$ value of $\Omega$, the adjusted LAI value became $LAI_r \cdot \Omega/0.7$. The leaf angle distribution (LAD) was fixed as erectophile, spherical, plagiophile, uniform, extremophile, and planophile. The canopy hotspot parameter ($S_l$), which is equal to the ratio of the correlation length of leaf projections in the horizontal plane and the canopy height, was fixed at 0.0001, 0.001, 0.01, and 0.1. I used these ranges of LAD and $S_l$ values to represent global distributions in these parameters. The solar incident zenith angle ($\theta_s$) was fixed at 25° for all model evaluations except when model sensitivity to this parameter was evaluated, and, in this case, $\theta_s$ was increased to 50°. The specular ratio to the total solar illumination ($r_{sd}$) was set at constant values representing typical atmospheric conditions on a clear day for each of the bands. I assumed that the error function of the atmospheric correction had an independent normal distribution with a mean of 0 and SD of $0.005 + 0.05\rho$ (no unit reflectance), where $\rho$ is the reflectance value at a given spectral band (Vermote and Kotchenova 2008).

In the calculation of each of combinations of the LAD and $S_l$ types, LAI values were provided from 0 to 10 at $10^{-6}$ intervals. I used pseudo-random numbers to express the lognormal and normal distributions of the leaf spectral parameters and soil reflectance. I calculated $10^7$ cases to obtain the relationships between $C_{ab}$, $C_m$, and $C_w$ and their associated spectral reflectances.

 

I used the TOA canopy spectral reflectance values at the MODIS green (545–565 nm; $R_G(\%)$), near infrared (841–876 nm; $R_{NIR}(\%)$), and shortwave infrared (1628–1652 nm; $R_{1640}(\%)$) bands to estimate $C_{ab}$, $C_m$, and $C_w$, respectively. The $R_G$, $R_{NIR}$, and $R_{1640}$ bands correspond to absorption bands of chlorophyll $a + b$, dry matter, and water and dry matter combined, respectively. Absorptions of carotenoids and anthocyanins also concern with $R_G$; however, in general, most of the leaf absorption at the green band corresponds to chlorophyll $a + b$. That was because the carotenoids concentration and $C_{ab}$ have a high positive correlation for a variety of plant species and the anthocyanins concentration appears when the leaves of deciduous trees turned red in autumn. For the estimation of $C_w$, the estimated $C_m$ value from $R_{NIR}$ was multiplied by the ratio of the specific absorption coefficient of water ($cm^2$ mg) to that of dry matter ($cm^2$ mg), which is 0.787, and then removed this value ($f_i(R_{NIR})$) from the estimated $C_w$ because the PROSPECT model shows that both $C_w$ and $C_m$ contribute to $R_{1640}$. For the estimation of $C_w/C_{ab}$, the estimated $C_w$ value was divided by the estimated $C_{ab}$ value.

I divided the ranges of the values of the TOA spectral reflectance or the abovementioned spectral indices into 8–12, and then calculated the average and SD of $C_{ab}$, $C_m$, $C_w$, and $C_w/C_{ab}$ for each of the divided ranges. To express the relationships in mathematical formulas for each of the estimated LAI value ranges, I used regression equations in the form:

$$y = ax^{-b}, \tag{2}$$

where $a$ and $b$ are constant values, $x$ is the spectral reflectance ($R_G$, $R_{NIR}$, or $R_{1640} + f_i(R_{NIR})$), and $y$ is the leaf constituent ($C_{ab}$, $C_m$, or $C_w$). For the ratio $C_w/C_{ab}$ for each of the estimated LAI value ranges, I used the regression equation in the form:

$$\frac{c_w}{c_{ab}} = a_1 {R_G}^{b1} {R_{1640}}^{-b2} - a_2 {R_G}^{c1} {R_{NIR}}^{-c2}, \tag{3}$$

where $a_1$, $a_2$, $b_1$, $b_2$, $c_1$, and $c_2$ were constant values. The coefficient of determination ($R^2$) was defined as:

$$R^2 = 1 - \frac{E^2}{SD^2}, \tag{4}$$

where $E$ is the root mean square error (RMSE) from the regression and SD is the standard deviation of the samples. Standard deviation for $C_{ab}$, $C_m$, $C_w$, and $C_w/C_{ab}$ was 16.4 $\mu$g $cm^{-2}$, 2.22 mg $cm^{-2}$, 5.63 mg $cm^{-2}$, and 0.174, respectively.

## Results

The LAI was estimated from the NDVI with $R^2$ of 0.39 for all combinations of the LAD and $S_l$ types together when $\theta_s = 25°$ (Fig. 1). The SD of the estimated LAI values over the intervals 0.95–1.05, 1.95–2.05, 2.95–3.05, 3.95–4.05, 4.95–5.05, 5.95–6.05, and 6.95–7.05 were 0.4, 0.9, 1.6, 2.1, 2.2, 2.1, and 1.8, respectively. Similarly, the LAI was estimated form the NDVI with $R^2$ of 0.30 when $\theta_s = 50°$.

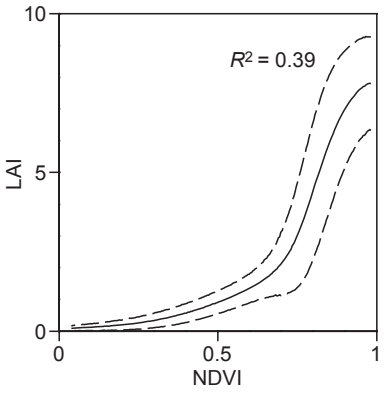


**Figure 1.** Relationship between normalized difference vegetation index and estimated leaf area index for all combinations of leaf angle distribution and $S_l$ types ($\theta_s = 25°$). The solid and dotted curves denote the average and the average ±SD, respectively, for each estimate.

I found a weak relationship between $C_m$ and $R_{NIR}$ and a strong relationship between $C_{ab}$, $C_w$, and $C_w/C_{ab}$ and their associated canopy spectral reflectances at the LAI values >2 when all the LAD and $S_l$ types were equally probable in one pixel of a remotely sensed image (Fig. 2). At the LAI values of 1, the $R^2$ of $C_{ab}$, $C_w$, and $C_w/C_{ab}$ estimations were <0.22. The LAI estimates of 2, 4, and 6 in Figure 2 correspond to the estimated LAI ranges of 1.95–2.05, 3.95–4.05, and 5.95–6.05, respectively.

However, for each of the estimated LAI ranges, as the LAD became more vertical or as $S_l$ decreased, $C_{ab}$, $C_m$, and $C_w$ decreased for the same canopy spectral reflectance values (Fig. 3). As the relationships between leaf constituents and associated canopy reflectances were dependent on the LAD and $S_l$ types, it was difficult to estimate $C_{ab}$ and $C_w$ from the canopy spectral reflectances when different LAD and $S_l$ types existed in the focal region of analysis. ${R_p}^2$ and ${R_e}^2$ in Figure 3 were the coefficients of determination under erectophile and $S_l = 0.0001$ parameterization and under planophile and $S_l = 0.1$ parameterization, respectively. In contrast, for the estimation of the $C_w/C_{ab}$ ratio, estimation equations were independent of the LAD and $S_l$ types (Fig. 3). The relationships between the estimated and observed $C_w/C_{ab}$ ratios for all combinations of the LAD and $S_l$ types (Table 1) fell within the two regression curves for erectophile and $S_l = 0.0001$ parameterization and for planophile and $S_l = 0.1$ parameterization (Fig. 3).

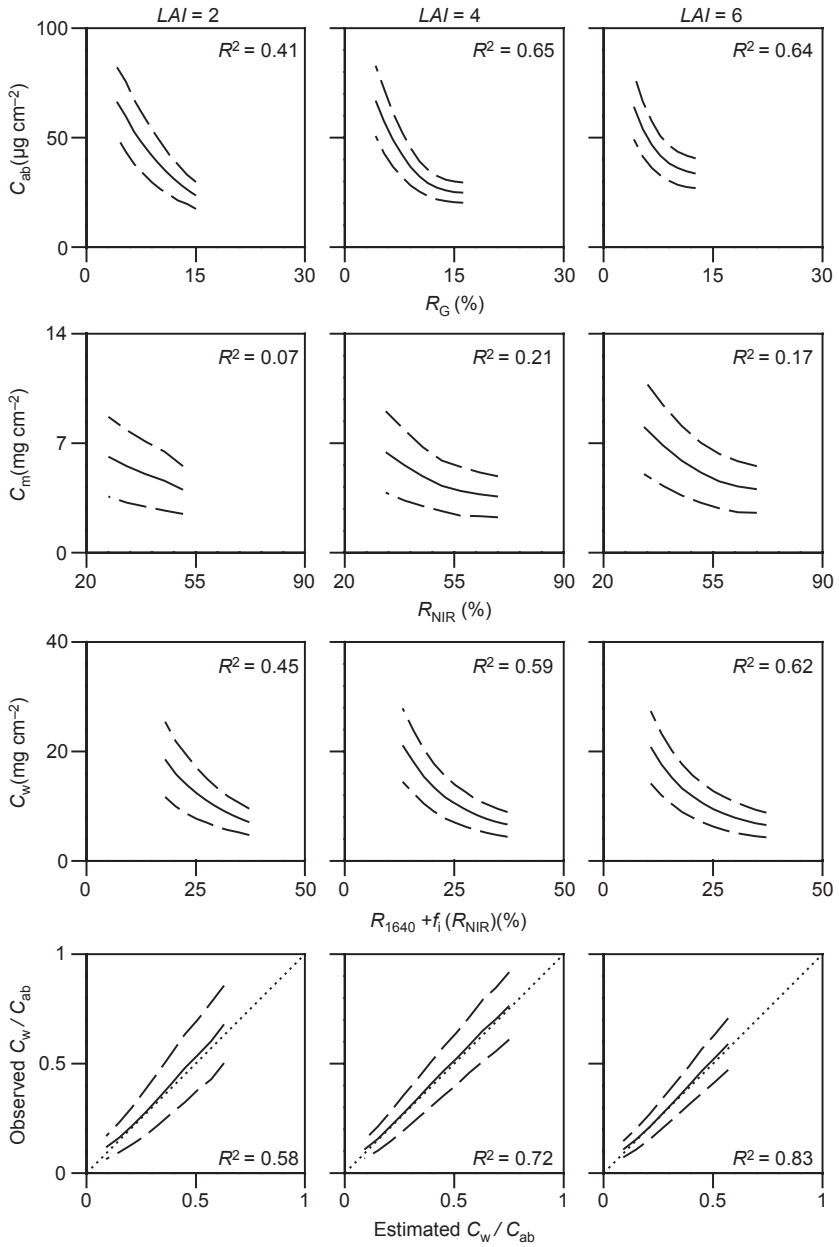


**Figure 2.** $R_G$ versus $C_{ab}$, $R_{NIR}$ versus $C_m$, $R_{1640}+f_i(R_{NIR})$ versus $C_w$, and estimated $C_w/C_{ab}$ versus observed $C_w/C_{ab}$ for all combinations of leaf angle distribution and $S_l$ types and for estimated leaf area indices of 2, 4, and 6 ($\theta_s$ = 25°). The solid and dotted curves denote the average and the average ±SD, respectively, for each estimate.

I found that the models were not sensitive to the value used for $\theta_s$. For an LAI value of 1, the $R^2$ of $C_{ab}$, $C_w$, and $C_w/C_{ab}$ estimates were <0.30, and the relationship between $C_m$ and the canopy spectral reflectance was weak. I could not estimate $C_{ab}$ and $C_w$ when different LAD and $S_l$ types existed in the focal region of analysis because the equations used to estimate $C_{ab}$ and $C_w$ were dependent on the LAD and $S_l$ types. However, the estimation equations for $C_w/C_{ab}$ were independent of the LAD and $S_l$ types. Coefficients of the regression equations of $C_w/C_{ab}$ for all combinations of LAD and $S_l$ types together in the form of equation (3) and the $R^2$ are shown in Table 2.

## Discussions and Conclusion

I evaluated global estimates of $C_{ab}$, $C_m$, $C_w$, and $C_w/C_{ab}$ from TOA broadband spectral reflectance using the PRO-

 

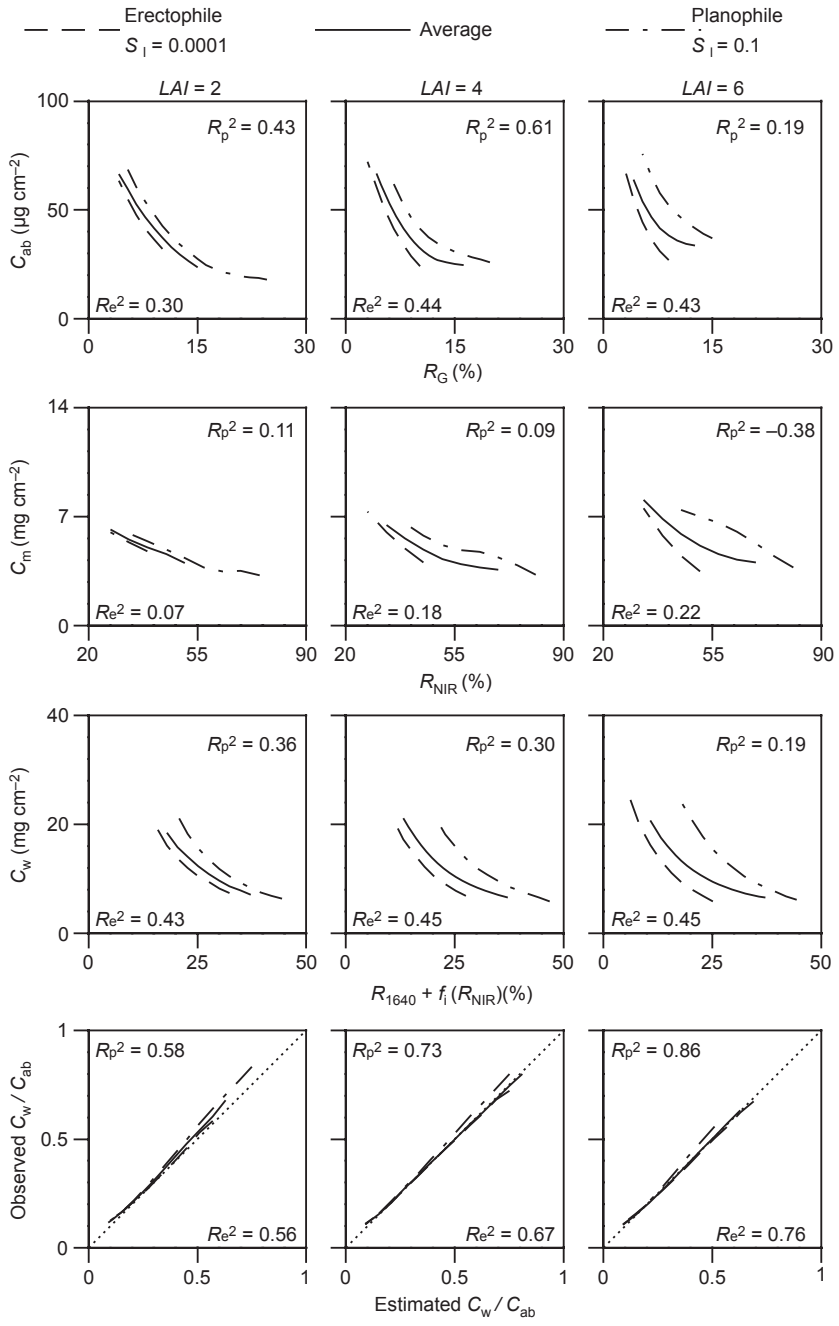


**Figure 3.** $R_G$ versus $C_{ab}$, $R_{NIR}$ versus $C_m$, $R_{1640}+f_i(R_{NIR})$ versus $C_w$, and estimated $C_w/C_{ab}$ versus observed $C_w/C_{ab}$ for estimated leaf area indices of 2, 4, and 6 ($\theta_s$ = 25°). Lines denote the averages of all combinations of leaf angle distribution (LAD) and $S_l$ types (solid lines), erectophile and $S_l$ = 0.0001 (dotted lines), and planophile and $S_l$ = 0.1 (dashed lines). $R^2_e$ represents $R^2$ when the LAD is erectophile and $S_l$ = 0.0001, and $R^2_p$ represents $R^2$ when LAD is planophile and $S_l$ = 0.1.

SAIL model for possible distributions of leaf and soil spectra, LAI, canopy geometric structure, and leaf size. For LAI values <2, $C_{ab}$, $C_w$, and $C_w/C_{ab}$ had weak relationships with their associated spectral reflectances. For LAI values greater than 2, $C_{ab}$ and $C_w$ could be reliably estimated only for certain ranges of LAD and $S_l$ types while the ratio of $C_w/C_{ab}$ could be reliably estimated for all possible canopy structures with an $R^2$ ranging from

**Table 2.** Coefficients of the equations for estimating $C_w/C_{ab}$.

| $\theta_s$ | $LAI$ | $a_1$ | $b_1$ | $b_2$ | $a_2$ | $c_1$ | $c_2$ | $R^2$ |
|---|---|---|---|---|---|---|---|---|
| 25 | 2 | 12.231 | 1.003 | 1.659 | 0.177 | 0.859 | 0.691 | 0.58 |
| | 3 | 8.660 | 0.949 | 1.541 | 0.349 | 0.858 | 0.847 | 0.67 |
| | 4 | 6.632 | 0.903 | 1.446 | 0.443 | 0.781 | 0.845 | 0.72 |
| | 5 | 5.392 | 0.866 | 1.373 | 0.665 | 0.682 | 0.876 | 0.77 |
| | 6 | 4.604 | 0.841 | 1.326 | 1.300 | 0.587 | 0.981 | 0.83 |
| | 7 | 4.179 | 0.784 | 1.286 | 3.604 | 0.529 | 1.208 | 0.89 |
| 50 | 2 | 12.120 | 0.978 | 1.645 | 0.239 | 0.898 | 0.785 | 0.61 |
| | 3 | 8.776 | 0.914 | 1.525 | 0.400 | 0.881 | 0.888 | 0.67 |
| | 4 | 6.745 | 0.870 | 1.430 | 0.532 | 0.807 | 0.900 | 0.73 |
| | 5 | 5.727 | 0.831 | 1.369 | 0.937 | 0.706 | 0.971 | 0.78 |
| | 6 | 4.932 | 0.810 | 1.327 | 2.136 | 0.614 | 1.117 | 0.84 |
| | 7 | 4.549 | 0.726 | 1.281 | 7.318 | 0.535 | 1.391 | 0.90 |

0.56 to 0.90. The estimation equation of $C_w/C_{ab}$ from the spectral reflectance and the $R^2$ value were dependent on the LAI values, but independent of the LAD and $S_l$ types.

Levels of $C_{ab}$, $C_m$, and $C_w$ can be indicative of leaf physiology and plant condition, and attempts have been made to estimate these values with remote sensing applications (Ustin et al. 2009). In previous site-specific studies, $C_{ab}$, $C_m$, and $C_w$ were successfully estimated using this methodology (Fourty and Baret 1997; Bowyer and Danson 2004; Zarco-Tejada et al. 2004, 2003; Gitelson et al. 2005; De Santis et al. 2006; Darvishzadeh et al. 2012; Si et al. 2012); however, the use of remote sensing to estimate these values at regional and global scales has not been reported. My research suggests that estimates of $C_{ab}$, $C_m$, and $C_w$ are dependent on LAD and $S_l$ types, and these types often vary across regional to global scales. As techniques for estimating LAD and $S_l$ types through remote sensing have not been established, a generalized estimation of $C_{ab}$, $C_m$, and $C_w$ across broad spatial scales is difficult except in cases where specific LAD and $S_l$ types can be inferred. In contrast, this study shows that the estimation of the $C_w/C_{ab}$ ratio through remote sensing techniques is generally possible across regional and global scales. The estimation of this ratio through remote sensing has not been previously considered as an indicator of plant canopy condition because the physiological meaning of the $C_w/C_{ab}$ ratio has been less well studied than those of $C_{ab}$, $C_m$, and $C_w$. However, I found that the $C_w/C_{ab}$ ratio had a stronger relationship with its associated spectral band than $C_{ab}$, $C_m$, and $C_w$ had to their associated bands.

Previous studies described the meaning behind and variations in $C_{ab}$, $C_w$, and $C_w/C_{ab}$. The value of $C_w/C_{ab}$ is specific to plant species, although, in general, the ratio slightly decreases with spring sprout and increases with autumn defoliation (Gond et al. 1999; Ceccato et al. 2001). For example, Scots pine, lodgepole pine, sun flowers, and sugar beets have high $C_w/C_{ab}$ values (1.0–1.8); poplars, oaks, and rhododendrons have moderate ratio values (0.5–0.7); and maize and rice have low values (0.1–0.2; Ceccato et al. 2001; Gond et al. 1999; Hosgood et al. 1995). The value of $C_w/C_{ab}$ also generally increases when a plant responds to stressors related to water deprivation (Zhang and Kirkham 1996; Guerfel et al. 2009), heat (Jeon et al. 2006), chilling (Bacci et al. 1996; Jeon et al. 2006; Korkmaz et al. 2010), high light conditions (Jagtap et al. 1998), ultraviolet rays (Alexieva et al. 2001), high salinity (Jaleel et al. 2008; Dogan 2011), and heavy-metal contaminants (Anuradha and Rao 2009). The increase in the ratio as a result of plant stress is caused by a greater decrease in leaf chlorophyll compared with leaf water.

Therefore, a change in the $C_w/C_{ab}$ ratio through time is the result of either changes in species composition or changes in the response of plants to stress. The former generally occurs at a yearly to decadal scale, whereas the latter occurs at a daily to monthly scale. Although disturbances such as wildfires, insect attacks, and deforestation can cause an immediate change in species composition, an analysis of changes in LAI and NDVI can help to distinguish between the causes of changes in $C_w/C_{ab}$. Thus, the remote estimation of the $C_w/C_{ab}$ ratio from satellites offers information on plant status at a global perspective.

Other than leaf chlorophyll $a + b$, leaf anthocyanins absorb the green light and generate the errors in the estimation of the $C_w/C_{ab}$ ratio. Leaf anthocyanins appear when the leaves of deciduous trees turned red in autumn or under chilling stress (Bacci et al. 1996). When a change in the estimated $C_w/C_{ab}$ ratio possibly appeared in such cases, an analysis of changes in the estimated LAI and NDVI can help to distinguish between the causes of changes in the estimated $C_w/C_{ab}$, as the autumn coloration reduces NDVI (Zhang et al. 2012).

This study modeled the global vegetation as to obey PROSAIL model with parameters shown in Table 1. The $R^2$ of the LAI estimation from NDVI with globally fixed equations were 0.30–0.39, whereas the $R^2$ of the $C_w/C_{ab}$ ratio estimation in the way I presented in this note was 0.56–0.90, for the estimated LAI values >2. This indicates that the global remote estimation of the $C_w/C_{ab}$ ratio is more reliable than that of LAI.

## Acknowledgments

I thank anonymous reviewers for their valuable suggestions. This study was supported by the Grant-in-Aid for Scientific Research (C), 20510001, 2008, from the Japan Ministry of Education, Science, Sports and Culture (MEXT) and the Arctic Research Projects using the

 

IARC-JAXA Information System of the Japan Aerospace Exploration Agency (JAXA).

## Conflict of Interest

None.

### References


Alexieva, V., I. Sergiev, S. Mapelli, and E. Karanov. 2001. The effect of drought and ultraviolet radiation on growth and stress markers in pea and wheat. Plant Cell Environ. 24:1337–1344.

Anuradha, S., and S. S. R. Rao. 2009. Effect of 24-epibrassinolide on the photosynthetic activity of radish plants under cadmium stress. Photosynthetica 47:317–320.

Bacci, L., F. Benincasa, and B. Rapi. 1996. Effect of growth temperature on the spectrocolorimetric characteristics of sorghum plants (*Sorghum bicolor* (L) Moench): indices of stress. Eur. J. Agron. 5:45–57.

Baldridge, A. M., S. J. Hook, C. I. Grove, and G. Rivera. 2009. The ASTER spectral library version 2.0. Remote Sens. Environ. 113:711–715.

Bowyer, P., and F. M. Danson. 2004. Sensitivity of spectral reflectance to variation in live fuel moisture content at leaf and canopy level. Remote Sens. Environ. 92:297–308.

Ceccato, P., S. Flasse, S. Tarantola, S. Jacquemoud, and J. M. Gregoire. 2001. Detecting vegetation leaf water content using reflectance in the optical domain. Remote Sens. Environ. 77:22–33.

Chen, J. M., C. H. Menges, and S. G. Leblanc. 2005. Global mapping of foliage clumping index using multi-angular satellite data. Remote Sens. Environ. 97:447–457.

Darvishzadeh, R., A. A. Matkan, and A. Dashti Ahangar. 2012. Inversion of a radiative transfer model for estimation of rice canopy chlorophyll content using a lookup-table approach. Selected Topics in Applied Earth Observations and Remote Sensing, IEEE Journal of PP:1–9.

Dogan, M. 2011. Antioxidative and proline potentials as a protective mechanism in soybean plants under salinity stress. Afr. J. Biotechnol. 10:5972–5977.

Fourty, T., and F. Baret. 1997. Vegetation water and dry matter contents estimated from top-of-the-atmosphere reflectance data: a simulation study. Remote Sens. Environ. 61:34–45.

Garrigues, S., R. Lacaze, F. Baret, J. T. Morisette, M. Weiss, J. E. Nickeson 2008. Validation and intercomparison of global leaf area index products derived from remote sensing data. J. Geophys. Res. Biogeosci. 113. doi: 10.1029/2007jg000635

Gitelson, A. A., A. Vina, V. Ciganda, D. C. Rundquist, and T. J. Arkebauer. 2005. Remote estimation of canopy chlorophyll content in crops. Geophys. Res. Lett. 32. doi: 10.1029/2005gl022688

Gond, V., D. G. G. de Pury, F. Veroustraete, and R. Ceulemans. 1999. Seasonal variations in leaf area index, leaf chlorophyll, and water content; scaling-up to estimate fAPAR and carbon balance in a multilayer, multispecies temperate forest. Tree Physiol. 19:673–679.

Guerfel, M., O. Baccouri, D. Boujnah, W. Chaibi, and M. Zarrouk. 2009. Impacts of water stress on gas exchange, water relations, chlorophyll content and leaf structure in the two main Tunisian olive (*Olea europaea* L.) cultivars. Sci. Hortic. 119:257–263.

Hosgood, B., S. Jacquemoud, G. Andreoli, J. Verdebout, G. Pedrini, and G. Schmuck. 1995. Leaf optical properties experiment 93 (LOPEX93). Technical report EUR 16095 EN. European Commission, Joint Research Centre, Institute for Remote Sensing Applications, Ispra, Italy.

Jacquemoud, S., and F. Baret. 1990. Prospect – a model of leaf optical-properties spectra. Remote Sens. Environ. 34:75–91.

Jacquemoud, S., W. Verhoef, F. Baret, et al. 2009. PROSPECT + SAIL models: a review of use for vegetation characterization. Remote Sens. Environ. 113:S56–S66.

Jagtap, V., S. Bhargava, P. Streb, and J. Feierabend. 1998. Comparative effect of water, heat and light stresses on photosynthetic reactions in *Sorghum bicolor* (L.) Moench. J. Exp. Bot. 49:1715–1721.

Jaleel, C. A., B. Sankar, R. Sridharan, and R. Panneerselvam. 2008. Soil salinity alters growth, chlorophyll content, and secondary metabolite accumulation in Catharanthus roseus. Turk. J. Biol. 32:79–83.

Jeon, M. W., M. B. Ali, E. J. Hahn, and K. Y. Paek. 2006. Photosynthetic pigments, morphology and leaf gas exchange during ex vitro acclimatization of micropropagated CAM Doritaenopsis plantlets under relative humidity and air temperature. Environ. Exp. Bot. 55:183–194.

Korkmaz, A., Y. Korkmaz, and A. R. Demirkiran. 2010. Enhancing chilling stress tolerance of pepper seedlings by exogenous application of 5-aminolevulinic acid. Environ. Exp. Bot. 67:495–501.

Kushida, K., and K. Yoshino. 2010. Estimation of LAI and FAPAR by constraining the leaf and soil spectral characteristics in a radiative transfer model. Int. J. Remote Sens. 31:2351–2375.

Running, S. W., R. R. Nemani, F. A. Heinsch, M. S. Zhao, M. Reeves, and H. Hashimoto. 2004. A continuous satellite-derived measure of global terrestrial primary production. Bioscience 54:547–560.

De Santis, A., P. Vaughan, and E. Chuvieco. 2006. Foliage moisture content estimation from one-dimensional and two-dimensional spectroradiometry for fire danger assessment. J. Geophys. Res. Biogeosci. 111. doi: 10.1029/2005jg000149

Si, Y., M. Schlerf, R. Zurita-Milla, A. Skidmore, and T. Wang. 2012. Mapping spatio-temporal variation of grassland


 

quantity and quality using MERIS data and the PROSAIL model. Remote Sens. Environ. 121:415–425.
Simard, M., N. Pinto, J. B. Fisher, and A. Baccini. 2011. Mapping forest canopy height globally with spaceborne lidar. J. Geophys. Res. Biogeosci. 116:G04021.
Ustin, S. L., A. A. Gitelson, S. P. Jacquemoud, M. Schaepman, G. P. Asner, J. A. Gamon, et al. 2009. Retrieval of foliar information about plant pigment systems from high resolution spectroscopy. Remote Sens. Environ. 113:S67–S77.
Verhoef, W. 1984. Light scattering by leaf layers with applications to canopy reflectance modeling. Remote Sens. Environ. 16:125–141.
Vermote, E. F., and S. Kotchenova. 2008. Atmospheric correction for the monitoring of land surfaces. J. Geophys. Res. Atmos. 113. doi: 10.1029/2007jd009662
Zarco-Tejada, P. J., C. A. Rueda, and S. L. Ustin. 2003. Water content estimation in vegetation with MODIS reflectance data and model inversion methods. Remote Sens. Environ. 85:109–124.
Zarco-Tejada, P. J., J. R. Miller, A. Morales, A. Berjon, and J. Aguera. 2004. Hyperspectral indices and model simulation for chlorophyll estimation in open-canopy tree crops. Remote Sens. Environ. 90:463–476.
Zhang, J. X., and M. B. Kirkham. 1996. Antioxidant responses to drought in sunflower and sorghum seedlings. New Phytol. 132:361–373.
Zhang, X. Y., M. A. Friedl, and C. B. Schaaf. 2006. Global vegetation phenology from moderate resolution imaging spectroradiometer (MODIS): evaluation of global patterns and comparison with *in situ* measurements. J. Geophys. Res. Biogeosci. 111. doi: 10.1029/2006jg000217
Zhang, X., M. D. Goldberg, and Y. Yu. 2012. Prototype for monitoring and forecasting fall foliage coloration in real time from satellite data. Agric. For. Meteorol. 158–159:21–29.

 